

# Influence of sea surface temperature on the European heat wave of 2003 summer. Part I: an observational study

Laura Feudale · Jagadish Shukla

Received: 21 September 2009 / Accepted: 5 March 2010  
© Springer-Verlag 2010

**Abstract** The heat wave affecting Europe during summer of 2003 is analyzed in detail with observational and reanalysis data. Surface, middle and upper troposphere analysis reveal particular circulation patterns related to an atmospheric blocking condition. In general seasonal anomalies, like this intense heat wave, are strongly related to boundary conditions. Composites and empirical orthogonal functions analysis provide evidence for an organized structure in the sea surface temperature (SST) anomaly field: high SSTs in the Mediterranean basin, the North Sea and further north toward the Arctic Circle were observed mainly in the months of June and August. The outcome of this analysis on observational data shows the SST as one of the possible factors in enhancing the heat wave in the European area.

**Keywords** Heat wave · Extreme 2003 summer · Europe · SST influence · Mediterranean

## 1 Introduction

The European heat wave of 2003 summer is considered to be one of the major climate anomalies in the extra-tropics in the recent times. It produced record-breaking temperatures in many cities of central-western Europe, of 38°C in London, 39°C in Milan and 42°C in Paris. This heat wave caused tragic deaths of more than 35,000 people and was responsible for many catastrophic socio-economic impacts, including enormous crop losses, forest fires and widespread persistent power losses (WHO 2003).

The surface temperature anomalies associated with this heat wave were more than five standard deviations in some parts of Europe (Schar et al. 2004). Model simulations indicate that hot summers could be more frequent in a future warmer climate, and therefore, the European heat wave of 2003 summer might give an indication of the nature of heat waves that can occur due to global warming (Schar et al. 2004; Beniston 2004; Meehl and Tebaldi 2004).

The Euro-Mediterranean region is of particular interest from the climate perspective since it represents a transitional zone between summer subtropical and extratropical regimes. Meridional migration of the latitude band in which baroclinic activity is more intense are associated with displacements of the intense subsidence accompanying the strong subtropical anticyclone. In both directions, these fluctuations regionally represent dramatic shifts in weather regimes. The occurrence of one of these shifts, caused by blocking, is generally related to hot events that interrupt the normal variability controlled by baroclinic eddies (Xoplaki et al. 2003; Cassou et al. 2005). However, notwithstanding the notion that the atmospheric flow associated with blocking may intuitively appear favorable to warm conditions, blocking alone is not sufficient to

---

L. Feudale (✉)  
The Abdus Salam International Centre for Theoretical Physics,  
Strada Costiera 11, 34151 Trieste, Italy  
e-mail: feudale@ictp.it

L. Feudale  
Center for Ocean-Land-Atmosphere Studies,  
Calverton, MD, USA

J. Shukla  
George Mason University, Fairfax, VA, USA

J. Shukla  
Institute of Global Environment and Society,  
Calverton, MD, USA

explain the amplitude and duration of certain heat waves. Even a canonical correlation analysis (CCA) by Della-Marta et al. (2007), demonstrating that heat waves have a well-defined multidecadal oscillation, substantially underestimates the amplitude of the 2003 wave, suggesting that other feedbacks are needed to produce an event of that magnitude. In addition to synoptic features such as favorable tropical Atlantic conditions acting as a forcing (Cassou et al. 2005), soil moisture (Ferranti and Viterbo 2006; Fischer et al. 2007), deficiency of precipitation (Vautard et al. 2006) and sea surface temperature (SST) anomalies along the European coasts and in the Mediterranean Sea (Feudale and Shukla 2007; Black and Sutton 2007; Jung et al. 2006) may significantly contribute to enhance the heat waves, making them also more persistent. In particular, the amplification of the heat wave and the SST anomalies in the areas surrounding the European region seems to have taken place interactively. Therefore, a valid hypothesis for intense heat waves is that both dynamical processes and feedback mechanisms in the free atmosphere and at the surface play a dominant role in accounting for the temporal variability of temperature and precipitation, which may lead to conditions favorable for extreme heat waves.

In this paper the primary goal is to analyze and explain the atmospheric circulation features associated with the heat wave of 2003 summer, evaluating also previous events that affected the same area, and showing the SST anomalies as one of the factors for the intensity and duration of the heat wave. The paper is organized as follows. Section 2 describes the data and Sect. 3 gives an observed description of the heat wave at the surface and upper troposphere; Sect. 4 identifies particular atmospheric patterns and SST anomaly structures with composites and Empirical Orthogonal Functions (EOFs) analysis. Section 5 discusses of possible mechanisms and Sect. 6 gives a summary and main conclusions.

## 2 Data

The gridded surface temperature data used in this analysis are provided by Pingping Xie from the National Centers for Environmental Predictions (personal communication). This dataset consists of a global, daily minimum ( $T_{\min}$ ) and maximum ( $T_{\max}$ ) surface temperature on a  $0.5^\circ$  grid, available from 1 October 1977 to the present. These data are analyzed from 6000 GTS stations on a near real-time basis. The algorithm used to create them is the same as that one used to define the precipitation described by Xie et al. (1996). The rainfall data are from Xie et al. (1996) and the soil moisture data from Fan and Van den Dool (2004). For the analysis of all the other atmospheric variables the

National Centers for Environmental Predictions-National Center for Atmospheric Research (NCEP-NCAR) Reanalysis data by Kalnay et al. (1996) are used. The historical Smith and Reynolds extended reconstructed SST dataset (Smith and Reynolds 2004) are used to analyze the variability and trend of SST during the past century and the OISST V2 data-set (Reynolds et al. 2002), linearly interpolated from weekly to daily, for the SST analysis on a daily time-scale during the spring and summer of 2003.

## 3 The 2003 summer European heat wave

### 3.1 Surface analysis

Several studies have documented the summer of 2003 as truly exceptional for record temperatures in many European cities (Schar et al. 2004), long persistence of high maximum daytime and minimum nighttime temperatures (Meehl and Tebaldi 2004), narrow day-night variations and exceptionally warm SSTs in the Mediterranean basin (Grazzini and Viterbo 2003). France, Switzerland, western Germany and northern Italy were the most affected countries by these record-breaking temperatures that exceeded the June–July–August (JJA) 1961–1990 mean by even as much as  $4\text{--}4.5^\circ\text{C}$  at the most (see Fig. 1). From a statistical point of view, the temperature reached up to five standard deviations (Schar et al. 2004), placing the event in the contest of an extreme, as pointed out by Schar et al. (2004), Beniston (2004) and more recently by Chase et al. (2006). Figure 2b shows that the European summer maximum temperature anomalies ( $T'_{\max}$ ) defined as departure from June to August 1980–2002 mean maximum temperature ( $\bar{T}_{\max}$ ), were above  $4^\circ\text{C}$ , with peaks of  $8^\circ\text{C}$  in the north-

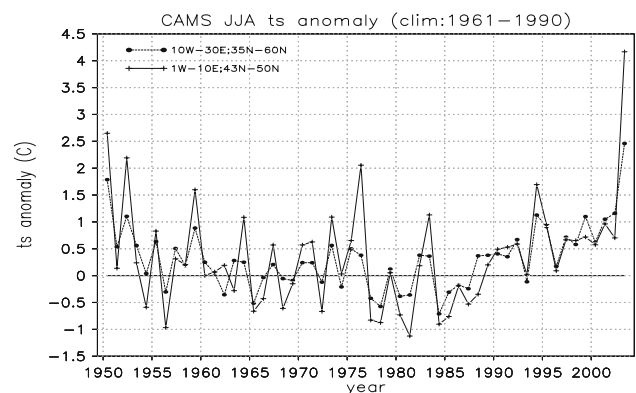


**Fig. 1** June–July–August (JJA) mean of CAMS surface temperature anomaly (with respect the climatology of the period 1961–1990) are averaged over the European area ( $10^\circ\text{W}\text{--}30^\circ\text{E}$ ,  $35\text{--}60^\circ\text{N}$ ) (solid line) and averaged over the area most affected by the heat wave ( $1^\circ\text{W}\text{--}10^\circ\text{E}$ ,  $43\text{--}50^\circ\text{N}$ ) (dashed line). The 2003 heat wave is on the top of the already increasing trend from 1985–2003. Units are in  $^\circ\text{C}$

western Europe, and the actual mean maximum temperature was about 28°C (Fig. 2a, b). The largest positive anomalies were observed in the months of June and August, especially in the southern part of France. From the time series of  $T_{max}$  over this region (Fig. 2c), averaged over the area (1°W–10°E, 43–50°N) shown as a box in Fig. 2b, the heat-waves in June and August may be easily identified. The figure shows that the maximum peak of the temperature anomalies in this region was reached during the first half of August with values above 10°C. The mean  $T'_{max}$  of the JJA season was above 4°C (the red line) and the mean of the daily-mean surface temperature anomaly was around 4°C, such that the 2003 summer heat-wave broke the record since at least 1950 (Fig. 1). Other studies indicate that 2003 summer was the warmest event

considering the period before 1950; Schar et al. (2004) using a long-term temperature series from Switzerland, located close to the center of the anomaly, showed that 2003 summer was the warmest since 1894 while Lutherbacher et al. (2004), using a multiproxy reconstruction of monthly and seasonal surface temperature fields and taking into consideration the reconstruction uncertainty, showed that 2003 summer appeared to be warmer than any other summer since 1500. The heat wave of 2003 summer had an unusually large spatial scale since a large part of Europe was affected.

Most European regions were subject to abnormally dry conditions in spring and particularly in summer of 2003 (Fig. 3a). The precipitation over Europe was below-normal, affecting the local soil moisture. The reduction of

**Fig. 2** JJA maximum air temperature at 2 m in the European region from the observed gridded Xie dataset: **a** JJA climatology (23 years period from 1980 to 2002); **b** JJA 2003 anomaly from the JJA climatology; the *rectangle* shows the most affected area by high temperatures; **c** time series of the temperature anomalies averaged over the area (1°W–10°E, 43–50°N) shown in figure **b**. Units are in °C

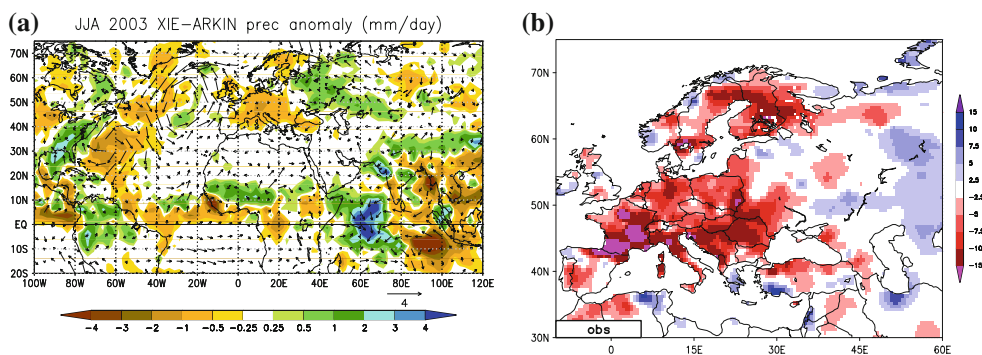
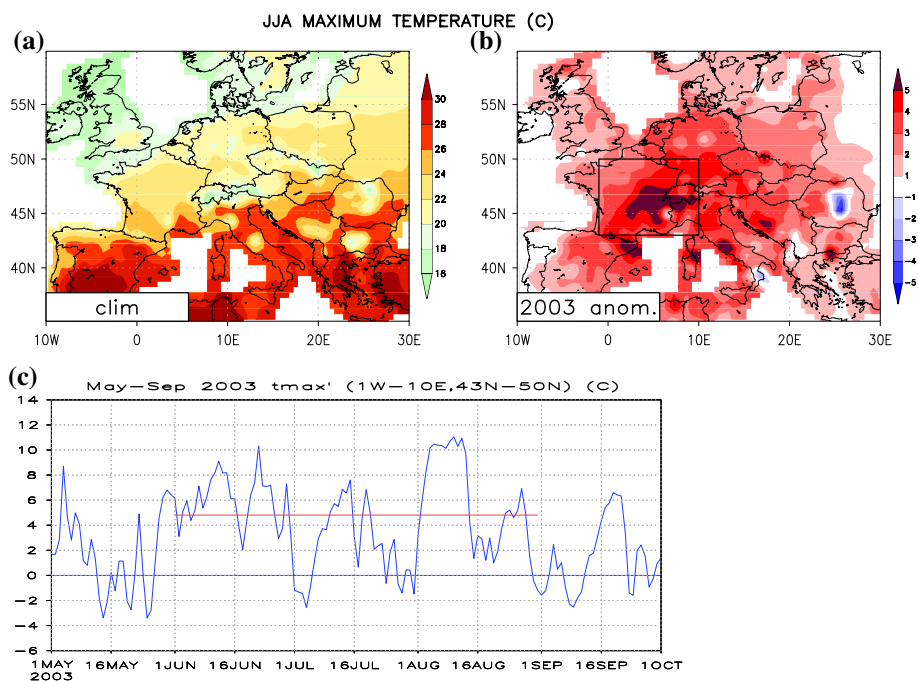


**Fig. 3** **a** Precipitation anomaly during JJA 2003 in color (mm/day) and vectors of wind anomaly (m/s) at 1,000 hPa height level from Xie Arkin data, and **b** JJA 2003 soil moisture anomaly (% of saturation): from Fan and Van den Dool (2004) dataset

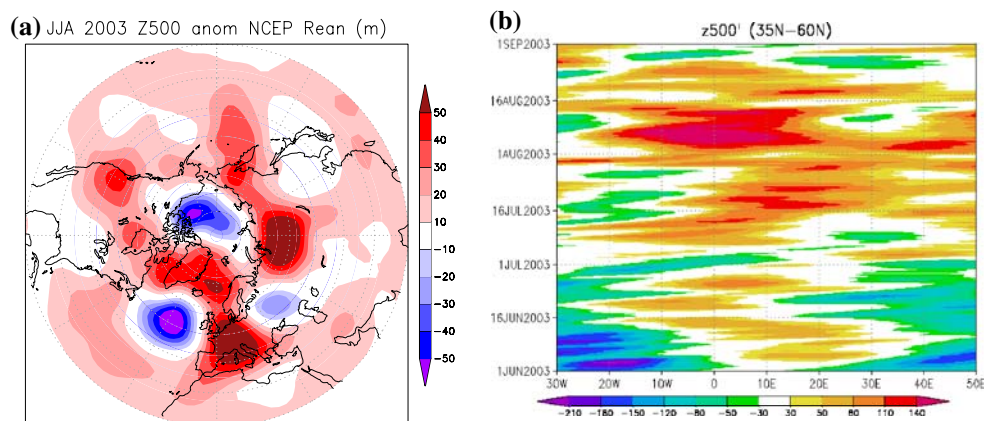


**Fig. 4** a JJA 2003 z500 anomaly and b Hovmöller diagram (time–longitude) section of z500 anomaly averaged over 35–60°N (m). NCEP reanalysis data

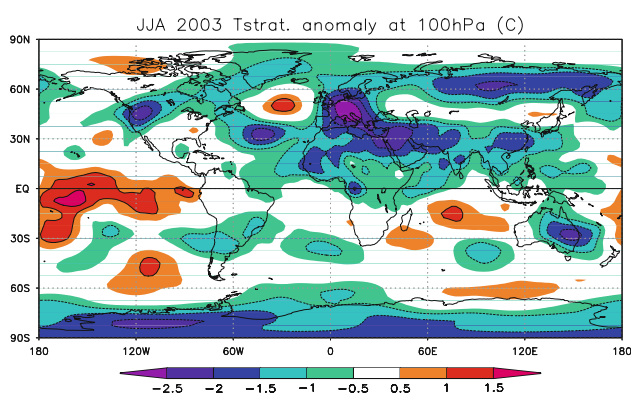


**Fig. 5** JJA 2003 lower stratosphere temperature anomaly (°C)

precipitation in the European area and the consequent deficit of soil moisture (Fig. 3b) could have further enhanced the heat wave. This has been further demonstrated in several studies (e.g. Ferranti and Viterbo 2006; Fischer et al. 2007). The African Intertropical Convergence Zone (ITCZ) shifted farther north, leading to an increase in precipitation in the western African Sahel (Fig. 3a). The increase in precipitation in the western African Sahel, as suggested by the study of Rowell (2003), might have been related to the warm Mediterranean SST.

### 3.2 Middle and upper troposphere analysis

The upper level circulation was characterized by a large positive geopotential height anomaly at 500 hPa height level (z500) over Europe during JJA (Fig. 4a), a cold anomaly in the lower stratosphere (Fig. 5) and a persistent blocking anticyclone. A Hovmöller (time–longitude) diagram of geopotential height anomaly at 500 hPa (z500') (Fig. 4b), latitudinally averaged over 35–60°N, shows the long persistence of large geopotential height anomalies

over the European region. A stationary wave between 20°W and 30°E persisted for the entire JJA season, except for a short break between the end of June and the beginning of July, and reached the maximum amplitude during August. The analysis of the vertical pressure velocity field at 500 hPa (Fig. 6a) indicates strong subsidence motion associated with the positive z500 anomalies during the peak in August. During this first part of August, the descending motion was much more enhanced preventing Atlantic storms from affecting any area inland of 5°W. Shaded in Fig. 6b is the vertical distribution of relative humidity (RH) zonally averaged over 5°W–35°E and the vectors represent the  $y$ - $p$  wind components, where the  $p$  component is the vertical pressure velocity multiplied by a factor of 100. Between 30 and 45°N, a region that includes the Mediterranean Sea, even though the RH at low levels was between values of 50–60%, the main meridional circulation was downward, and no convection occurred. The strong geopotential height anomaly at 500 hPa and the anomalous descending motion further north than usual were consistent with the northward shift of the ITCZ, leading to a northward shift of the descending branch of the Hadley cell and reduction in baroclinic activity (storm tracks) in the north.

### 3.3 Sea surface temperature analysis

The SST field with the OISST V2 data set (Reynolds et al. 2002) shows large SST anomalies (up to 3°C) during the summer of 2003 in the Mediterranean basin, the northern part of the North Atlantic Ocean, the North Sea and Norwegian Sea (Fig. 7). The tripole structure of SST anomaly in the northern Atlantic suggests an important role of air–sea interaction associated with the northward shift of the subtropical high (Huang and Shukla 2005; Czaja and Frankignoul 2002).



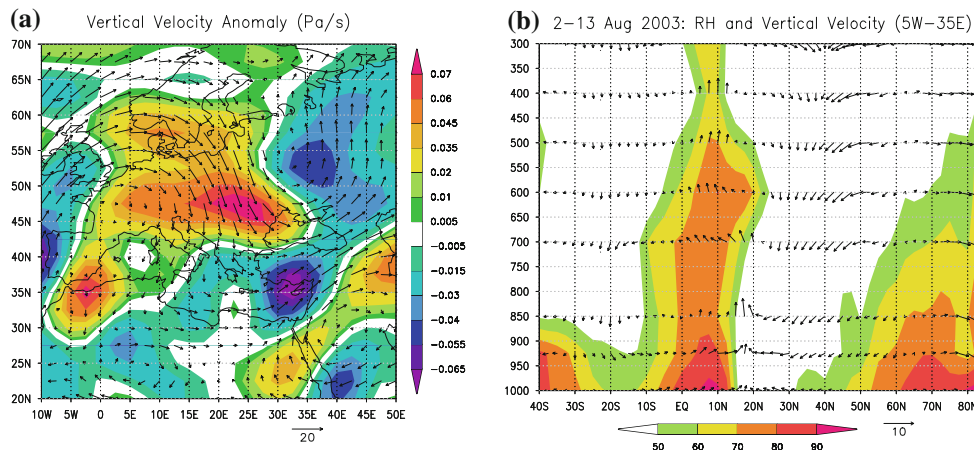
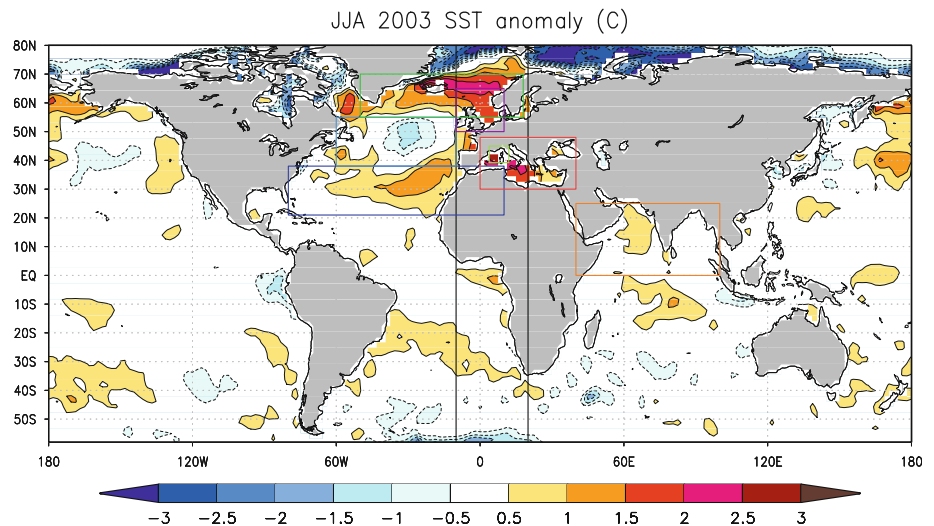


**Fig. 6** Vertical  $p$ -velocity ( $\omega$ ) during the peak of the heat wave (2–13 August 2003); **a** shaded contours show the vertical  $p$ -velocity ( $\omega$ ) anomaly showing the area over Europe where the subsidence motion was above normal ( $\text{hPa s}^{-1}$ ); the vectors show the wind direction at

500 hPa height level; **b** pressure–latitude ( $y$ – $p$ ) section of relative humidity (RH) averaged from 5°E to 35°W for August 2–13. Contour interval is 10. The vectors show the vertical–meridional velocity. The vertical motion has been multiplied by 100

**Fig. 7** JJA 2003 SSTA (°C). The colored rectangles show the regions analyzed in Fig. 9. The vertical lines indicate the domain for the analysis displayed in Fig. 13. (OISST-V2 data, Reynolds et al. 2002)



The warmest values were recorded in the north-western part of the Mediterranean Sea. A time series of JJA SSTA averaged over the Mediterranean basin and Black Sea (6°W–42°E, 30–48°N), calculated with respect to 1961–1990 mean, shows that SST in this area was warmer than previous summers since 1854 and that its value was outside the range of variability in the previous 150 years (Fig. 8). Starting from the 1990s, the growth is quite noticeable, reaching the highest value of about 1.5°C in 2003. Comparing the time series of the Mediterranean SST with the time series of the surface temperature in Europe in Fig. 1 during 1950–2003, it is seen that both sea and land surface temperatures had a positive trend since late 1980s. Monthly maps of SST just in the Mediterranean Sea (not shown here) had a positive anomaly almost everywhere but not uniformly distributed. The most affected part was in the north-west (Fig. 7) where  $T'_{\max}$ , after reaching the

maximum value in June, persisted above 2°C until the end of August. Using the OISST V2 data set (Reynolds et al. 2002), after a linear interpolation from weekly to daily, the SSTA evolution was analyzed on the daily time scale during the spring and summer of 2003. Figure 9 shows the time series of daily SSTAs from March to the end of September in regions that might have influenced the European climate either directly or through teleconnections. The analyzed regions are shown in Fig. 7 with the same colors as the respective time series of Fig. 9. A noticeable warm SSTA built up rapidly in the western Mediterranean Sea starting from the second half of April (light-green line). After a slow decrease in the middle of May, the anomaly grew further in the first two weeks of June, after which it reached the maximum value of 4°C. The red line represents the time series of SSTA averaged over the entire Mediterranean basin and Black Sea. There

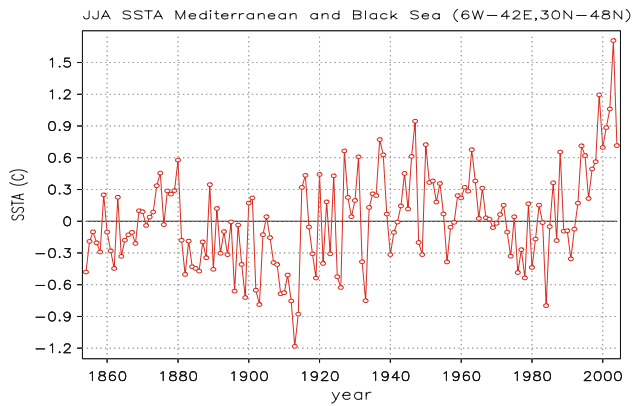


**Fig. 8** JJA 1854–2004 time-series of SST anomalies in the Mediterranean and Black Sea ( $6^{\circ}\text{W}$ – $42^{\circ}\text{E}$ ,  $30^{\circ}$ – $48^{\circ}\text{N}$ ) calculated with respect to the 30-year (1961–1990) climatology using the Historical Smith and Reynolds extended reconstructed SST dataset (Smith and Reynolds 2004)

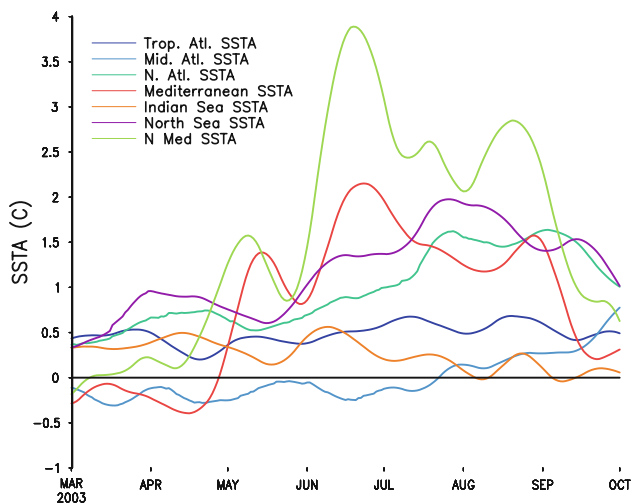


**Fig. 9** SSTA time-series from March to October 2003 in the following areas ( $^{\circ}\text{C}$ ): Tropical Atlantic Sea ( $80^{\circ}\text{W}$ ,  $10^{\circ}\text{E}$ ;  $21^{\circ}\text{N}$ ,  $38^{\circ}\text{N}$ ); Mid North Atlantic Ocean ( $60^{\circ}\text{W}$ ,  $10^{\circ}\text{W}$ ;  $38^{\circ}\text{N}$ ,  $55^{\circ}\text{N}$ ); Top North Atlantic Ocean ( $50^{\circ}\text{W}$ ,  $18^{\circ}\text{E}$ ,  $55^{\circ}\text{N}$ ,  $70^{\circ}\text{N}$ ); Mediterranean Sea ( $0^{\circ}$ ,  $40^{\circ}\text{E}$ ;  $30^{\circ}\text{N}$ ,  $48^{\circ}\text{N}$ ); Indian Ocean ( $40^{\circ}\text{E}$ ,  $100^{\circ}\text{E}$ ;  $0^{\circ}\text{N}$ ,  $25^{\circ}\text{N}$ ); North Sea ( $10^{\circ}\text{W}$ ,  $10^{\circ}\text{E}$ ;  $50^{\circ}\text{N}$ ,  $65^{\circ}\text{N}$ ); Genoa Gulf ( $3.8^{\circ}\text{E}$ ,  $12^{\circ}\text{E}$ ,  $39.2^{\circ}\text{N}$ ,  $45^{\circ}\text{N}$ )

was a lag of few days with respect to the north western part (light-green line), and the anomaly reached the maximum amplitude of  $2^{\circ}\text{C}$  in the middle of June and remained positive for the entire duration of the summer. Thus, the Mediterranean Sea, which usually cools due to storms in normal years, did not cool down at all. In spite of warmer SSTs and greater evaporation, a strong anticyclone persisting over the entire Euro-Mediterranean area suppressed deep convection and contributed to *reduced* rainfall.

The SSTAs in the northern part of the North Atlantic Sea and the North Sea also had a gradual positive trend during the summer, reaching the maximum between the

end of July and beginning of August (Fig. 9). The maximum of the North Sea SSTA preceded that of the north western Mediterranean Sea suggesting a possible “atmospheric teleconnection” between the two areas. The North Sea SSTA could have produced the atmosphere circulation which inhibited cooling of the Mediterranean by storms. The time series of the Indian Ocean SSTA (the orange line in Fig. 9) followed the Mediterranean SSTA trend, although the maximum amplitude reached during mid-June was only about  $0.5^{\circ}\text{C}$ . A link between the heat wave and the Indian Ocean anomalies was already proposed by Black and Sutton (2007), who suggested that the Indian Ocean warming might have contributed to the persistence of the temperature and precipitation anomalies over Europe during the month of August. The middle North Atlantic Ocean (light-blue line), in contrast, developed a colder anomaly lasting through the end of July followed by a smaller warm anomaly. The cold anomaly was related to the wind stress associated with the strong cyclonic circulation in that area (Fig. 3a). The Tropical Atlantic Ocean (dark blue line) was persistently warm around  $0.5^{\circ}\text{C}$ .

## 4 Pattern identification

### 4.1 Heat wave composites

In order to examine more comprehensively the dynamical evolution and features associated with heat waves in the European area, composites of various surface and dynamical fields were calculated for major warm events. Using the method described by Feudale (2008), the major warm events that occurred between 1950 and 2003 in the European area of  $35^{\circ}$ – $70^{\circ}\text{N}$ ,  $11^{\circ}\text{W}$ – $69^{\circ}\text{E}$  were selected. Among these, the first nine major events were used for calculating

**Table 1** List in chronological order of nine major warm events occurred in western Europe during summers 1950–2003: the first column lists the days of persistence, the second and the third columns list the onset and the end of the heat wave respectively

Duration (days)	Start time	End time
17	24 Jun 1952	10 July 1952
15	23 Jun 1976	7 July 1976
16	7 July 1983	1 August 1983
16	16 August 1992	31 August 1992
31	18 July 1994	17 August 1994
15	30 July 1998	13 August 1998
23	9 August 2000	23 August 2000
31	13 Jun 2002	2 July 2002
33	6 Jun 2003	8 July 2003

the composites and are chronologically listed in Table 1 with the respective days of persistence.

The composite of  $T'_{\max}$  (Fig. 10a) shows that, in the main affected area of  $10^{\circ}\text{W}$ – $35^{\circ}\text{E}$ ,  $35$ – $55^{\circ}\text{N}$ , the daily mean maximum surface temperature increases above  $5^{\circ}\text{C}$  with respect to the normal. At the same time, another common but less intense positive maximum temperature anomaly is noticeable over Siberia.

The composite of SSTAs (Smith and Reynolds 2004) with respect to 1961–1990 for the same summer month and year of the events (Fig. 10b) does not show any large SSTA over the global oceans. However, positive SST anomalies occur in the Mediterranean Sea at least  $0.5$ – $1^{\circ}\text{C}$  above the climatological mean. Also the North Sea has warmer SST. The absence of a large SSTA over the global oceans suggests that there is no preferred SSTA pattern responsible for the European heat waves. Yet, it does not rule out the possibility that an individual heat wave is indeed affected by SST anomalies. The composite of z500 anomalies (Fig. 10c) shows that the central-western European region during a heat wave is characterized by a persistent blocking anticyclone and may be responsible for the heat waves' persistence and intensity. In agreement with the positive anomaly of z500 and a warm anticyclone at the surface, the composite of temperature anomaly in the lower part of the stratosphere at 100 hPa (Fig. 10d) shows a negative anomaly, implying a stratosphere cooling.

As further evidence that seasonal anomalous heat waves are usually strongly related with boundary conditions (BCs) (Goddard et al. 2001), observations and composite analyses support the idea that a given global SSTA pattern can help to set up the specific atmospheric circulation pattern for a heat wave. Large local SSTAs may have strong influence on the local and large hemispheric circulation. For 2003 summer, further analysis described in the following section supports this assessment.

#### 4.2 EOFs analysis and weather regimes

EOFs have been computed for maximum surface temperature to determine the areas most affected by the heat waves during the summer of 2003. A regression analysis is then applied on the Principal Components (PCs) to identify possible relations with particular atmospheric patterns and SST patterns.

The EOF analysis is calculated in the area ( $12^{\circ}\text{E}$ – $35^{\circ}\text{W}$ ,  $30$ – $60^{\circ}\text{N}$ ) in the time-window between 1 April and 30 September in order to capture the main changes in the temperature field affecting the European area. The leading EOF that accounts for 23.4% of total variance and the corresponding PC (Fig. 11a, b) show that extended area of Europe (central, eastern and southern part) are affected by very warm temperatures during the first half of June, second half of July and first half of August. The second EOF

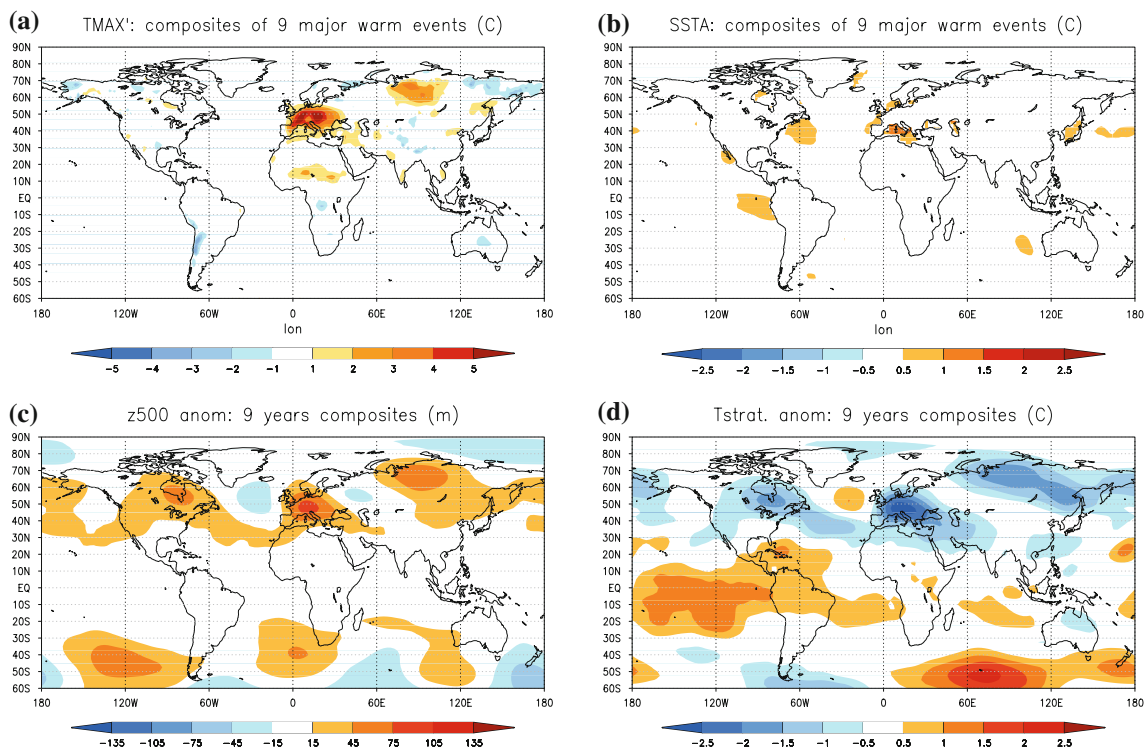


**Fig. 10** Composites of the nine major warm events listed in Table 1 occurring in the central–western Europe between 1950 and 2003: **a**  $T'_{\max}$  ( $^{\circ}\text{C}$ ); **b** SSTA ( $^{\circ}\text{C}$ ); **c**  $z500'_{\max}$  (m); **d** lower stratosphere temperature anomaly (at 100 hPa) ( $^{\circ}\text{C}$ )

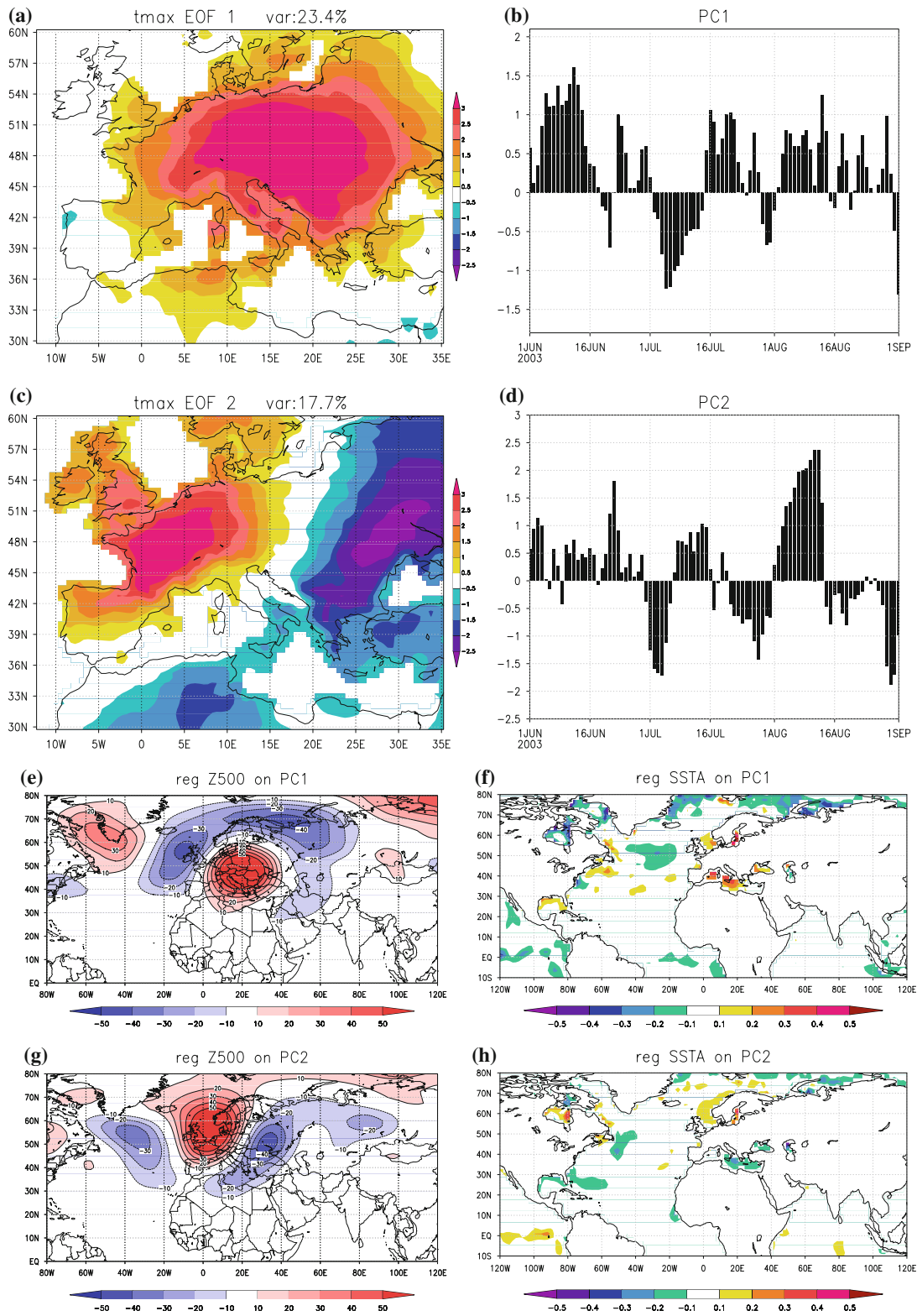


**Fig. 11** EOF components calculated between 1 April 2003 and 30 September 2003 in the area (12°E–35°W, 30–60°N): leading (a) EOF and (b) PC; second (c) EOF and (d) PC. Regression analysis of (e)

$z500'_{max}$  and (f) SSTA on the first PC; (g) and (h) the same as (e) and (f) only for the second PC



and PC (Fig. 11 c, d), that accounts for 17.7% of total variance, identifies central-western Europe as the area most affected by the warmest temperature occurring during the first half of August. In fact, France and southern England were the most affected (WHO 2003).

The response for this anomalous warming in relation to a particular atmospheric pattern (or vice versa) is derived by the use of regression coefficient in dealing with the PC and the z500 field in the same time frame. The regression of the z500 field on the PC of the leading mode results in an Atlantic Low pattern (as in Cassou et al. 2005) with a positive z500 anomaly centered right over Europe. This atmospheric circulation regime lasted for the most part of June, second half of July and dominated during August. The second EOF which has the peak in the first half of August is seen to be related to a persistent blocking condition with a strong positive z500 anomaly centered over the North Sea. This is consistent with the results found by Cassou et al. (2005).

EOFs are also directly calculated for the z500 anomaly field to identify the particular weather regimes during that summer. The first and second EOFs account for 14.6 and 13.1% of the total variance, respectively. The leading mode (Fig. 12a, b) represents a sort of blocking condition that affects both Europe and Russia and shows its peak during the mid half of August, similar to what was found in the previous regression analysis calculation. The second component (Fig. 12c, d) shows a dominant Atlantic Low during most part of June and a positive z500 anomaly right over central Europe. The positive z500 anomaly from central-southern Europe then shifts northward to settle in a blocking condition up to the middle of August.

SST is linearly regressed on the first and second PCs to identify which SST pattern occurs simultaneously with the event. The leading mode is related through a warm SST anomaly in the north/central Mediterranean Sea, North Sea and Baltic Sea and a cold anomaly in the central North Atlantic Ocean (Fig. 11e, f). The second pattern is related

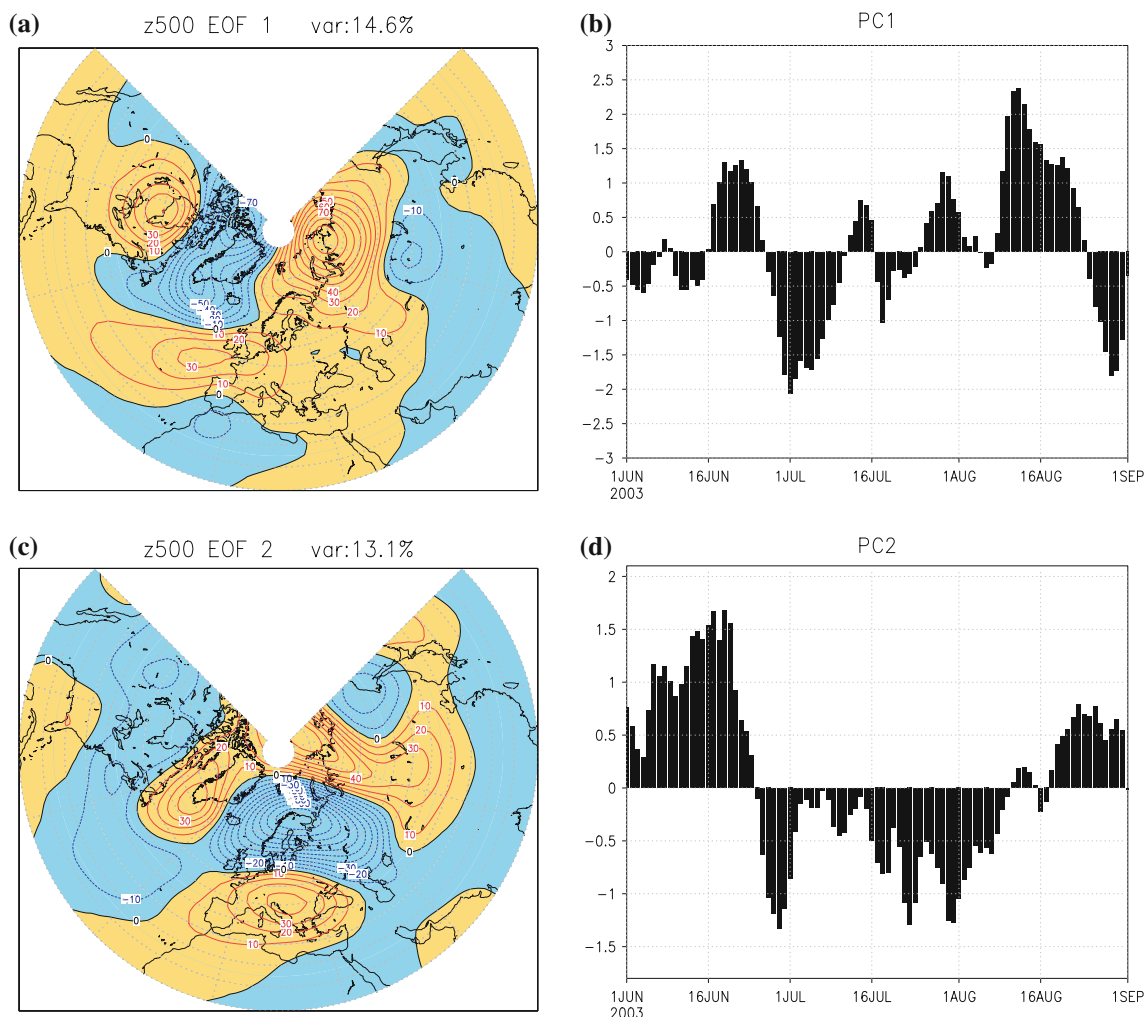


**Fig. 12** EOFs of z500 anomaly between 1 April 2003 and 30 September 2003 calculated in the area (120°W–150°E, 20–85°N): (a) and (b) first EOF and PC; (c) and (d) second EOF and PC

just to the warm anomaly in the North Sea and Baltic Sea (Fig. 11g, h). These conclusions support the results from the composite analysis that showed a relation between the warm land surface with the surrounding warm sea surfaces and the large atmospheric blocking. The hypothesis of a possible relation and/or feedback generated by global anomalies of SST to the land surface temperature during the summer of 2003 is tested with the COLA AGCM in Feudale and Shukla (2010).

## 5 Discussion

Both middle and upper troposphere analysis and EOFs analysis show that this intense heat wave is associated with an anomalous atmospheric circulation over the North Atlantic Ocean leading to a blocking situation, a result

supported by studies of Cassou et al. (2005) and Della-Marta et al. (2007). The tripole structure of SST anomaly (Fig. 7) suggests that the initial growth of Atlantic SST anomalies may be related to atmosphere–ocean interaction associated with shifts in circulation over the Atlantic. The amplification of the heat wave and the Atlantic SST anomalies also seems to have taken place interactively. The modeling study by Cassou et al. (2005) suggests a forcing mechanism in which a northward migration and intensification of the Atlantic ITCZ with an enhanced African Monsoon which in turn induces reinforced sinking motion over southern Europe. Ogi et al. (2005) uses EOFs to demonstrate the abnormal amplitude of the 2003 summer Northern Hemisphere Annular Mode (summer NAM). They show that extremely high values persisted from late July for at least 2 weeks, in correspondence with the heat wave in Europe. During a large positive phase of the

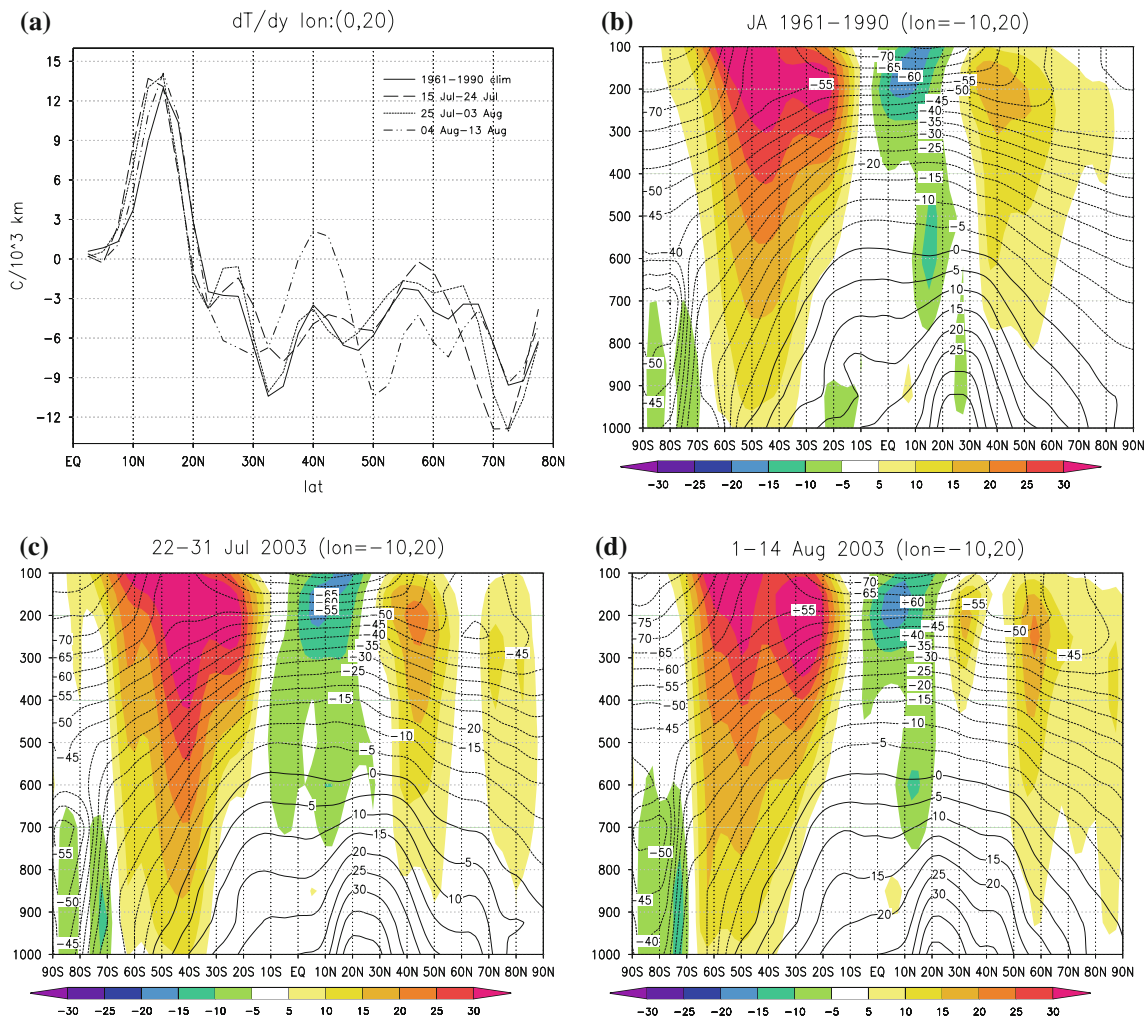


**Fig. 13** **a** Meridional gradient of zonal ( $10^{\circ}\text{W}$ ,  $20^{\circ}\text{E}$ ) temperature during July–August (JA) 2003 calculated using the 30-year reference period and the 10-day step from July 15 to August 13. **b** In solid line, the vertical section of JA 30-year temperature zonal averaged

between ( $10^{\circ}\text{W}$ ,  $20^{\circ}\text{E}$ ) and, shaded, the zonal wind in the same section ( $\text{m s}^{-1}$ ); isotherm distance of  $5^{\circ}\text{C}$ . **c** The same as **(b)** only for the 22–31 July 2003; **(d)** The same as **(b)** only for the 1–14 August 2003

summer NAM, usually a double-jet structure (a polar and a subpolar jet stream) appears in the upper troposphere (Ogi et al. 2004). The double-jet structure for this event can be inferred in Fig. 13c, d. This pattern usually tends to cause atmospheric blocking that stops the eastward propagation of cyclones and thereby supporting the long-lasting weather anomalies.

From the composite analysis (Fig. 10), common circulation features of the European heat waves consist of positive geopotential height anomalies and anomalous anticyclonic circulation over Europe, which produce large scale descending motion, decreased convection and increased incoming solar radiation and lead to warmer Mediterranean SST. Anomalous low level circulation prevents the lee waves and cyclones associated with topographic effects (Buzzi and Tibaldi 1978) to cool the Mediterranean by wind-induced mixing, thereby further warming the SST. Thus, the combined effects of increased incoming solar radiation and lack of upper ocean mixing due to absence of storms can produce warmer Mediterranean SST. The SST anomaly composite of nine major European heat waves shows the warmest SST anomalies over the Mediterranean. This, of course, does not necessarily mean that the Mediterranean SST anomalies influence the European heat waves. In fact, it is far more reasonable to argue that the warmer Mediterranean SST is an integral part of the European heat waves.

The simultaneous occurrence of warmer SST in the North Sea and the surrounding northern part of the North Atlantic Ocean (results from both composites and EOFs analysis) suggest an important SST effect in the Mediterranean area. The effect can be explained as a reduction in baroclinicity and preventing baroclinic waves to influence the Mediterranean area. In fact, the warm SST in the North Sea and the surrounding areas in the North Atlantic Ocean reduces the meridional gradient of temperature ( $dT/dy$ ) between the continental Europe and the North Sea. This

mechanism leads to a reduction of the baroclinic instability over the European–Mediterranean area and a northward shift of the North Atlantic storm track. Figure 13a shows  $dT/dy$  zonally averaged over  $10^{\circ}\text{E}$ – $20^{\circ}\text{W}$  in order to include the entire central-western Europe. The July–August climatology of  $dT/dy$  calculated for the 30-year period (1961–1990) is shown in solid line. The  $dT/dy$  calculated every 10 days between 15 July and 13 August 2003 (i.e., 15–24 July, 25 July–03 August, 04–13 August) are represented by the dashed, dotted and dash-dotted lines, respectively. It is shown that, from the middle of July to the beginning of August (15–24 July and 24 July–03 August of 2003), the  $dT/dy$  over  $50$ – $70^{\circ}\text{N}$  gets smaller in absolute value than the climatological values, getting close to zero. In the vertical profile of the zonally averaged temperature shown in Fig. 13c, the atmosphere between continental Europe and the North Sea ( $50$ – $70^{\circ}\text{N}$ ) looks almost barotropic, with practically no vertical wind shear. Thus the baroclinic instability, typical of these latitudes (see Fig. 13b), is reduced.

The decrease of baroclinic activity is further proven by the negative Eddy Kinetic Energy (EKE) anomaly at 250 hPa (Fig. 14a, b) from the middle of July in the northern part of the North Atlantic Ocean. Baroclinic instability is considered to be a limiting factor that prevents the northward expansion of the northerly branch of the Hadley cell. If this instability is reduced, the descending branch of the Hadley cell may expand northward. Moreover, intense baroclinic activity means generation of cyclones that can reduce the area of high pressure. If the meridional gradient of temperature diminishes, the northerly branch of the Hadley cell may expand northward, and the absence of cyclonic activity will help the anticyclonic circulation to persist. The dominant downward motion (Fig. 6a, b) increases the pressure in the lower levels initiating processes that warm up the land and the surrounding sea surface, especially due to a decrease in cloudiness and

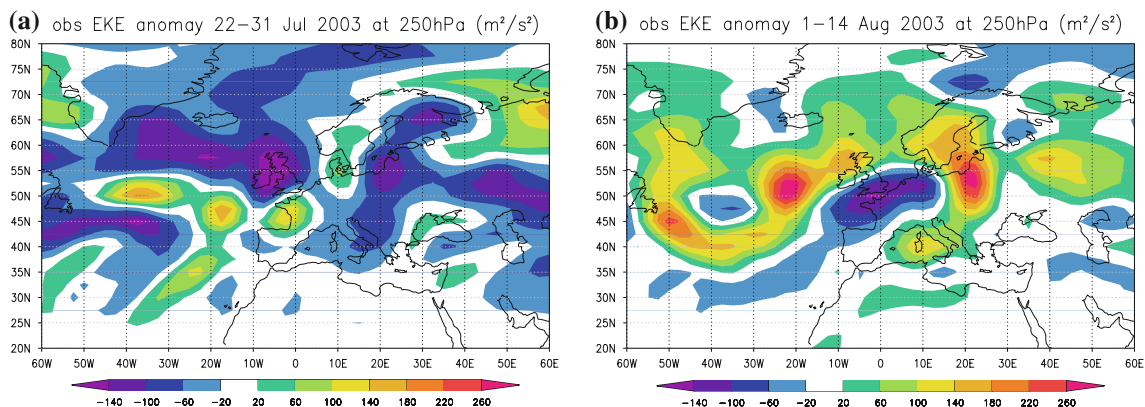


**Fig. 14** Eddy kinetic energy anomaly at 250 hPa (a) 10 days before the onset of the major heat wave (the 22–31 July 2003 period) and (b) during the heat wave in the period of time 1–14 August 2003 ( $\text{m}^2 \text{s}^{-2}$ )

an increase in downward solar radiation. In spite of the warm Mediterranean SST that may create convection, the dominant descending motion prevents the convection and create a cloud-free sky (as the images taken from satellite at <http://www.sat.dundee.ac.uk> show), leading to an increase in downward solar radiation. During August 2003, an increase of 20% of incoming solar radiation with respect to the normal was observed (Albuisson et al. 2003), resulting in an increase of the temperatures at lower levels. This situation persists and becomes more and more intense as long as the “area of reduced baroclinic activity” prevents baroclinic waves to penetrate inland and in to the Mediterranean area.

During the first half of August, the entire Euro-Mediterranean area became warmer (both sea and land surface). Figure 13d shows that, at the beginning of August, the “barotropic atmosphere”, generated during the end of July between continental Europe and North Sea, moves to lower latitudes of 30–45°N leading the  $dT/dy$  gradient close to zero (dash-dotted line in Fig. 13a). The vertical profile of Fig. 13d reflects the double-jet structure that may support the blocking situation, as explained by Ogi et al. (2004).

## 6 Summary and conclusions

In this study the authors have analyzed the heat wave of the 2003 summer in Europe and investigated the influence of SST by analyzing observational data to identify possible precursors. The analysis has shown a large anticyclonic anomaly over Europe, large SSTAs in the Mediterranean Sea (up to 4°C in the western part) and in the North Sea and also positive SSTAs in the Indian Ocean since January. The African ITCZ shifted northward with a strengthening of the vertical circulation emphasized by a cold anomaly in the lower stratosphere. It appears that the warm SSTA in the northern part of the North Atlantic Ocean, toward the Arctic Circle, affected the air temperature field in the mid-high latitudes, right above the European area, leading to a reduction of the absolute value of the meridional gradient and a consequent decrease of the baroclinic activity in that area. This resulted in a northward shift of the polar jet, allowing the expansion of the anticyclone over the central Europe.

Observations have also shown large negative soil moisture anomalies since early spring due to a reduction in precipitation. An increase of rainfall observed over the western African Sahel, may be related to the warm Mediterranean SST as explained by Rowell (2003).

Composites and EOF analysis have provided evidence for an organized structure in the SST anomaly field. In Feudale and Shukla (2007), the effects of just Mediterranean SST alone was analyzed and it was shown that while

Mediterranean SST anomalies are not responsible to produce the heat wave, once a heat wave is initiated, warm Mediterranean SST anomalies reinforce the heat wave. From the present study it is found that not only the Mediterranean Sea developed strong SST anomalies, but also the North Sea and the surrounding parts of the North Atlantic. Therefore additional experiments with an atmospheric global circulation model are necessary to investigate further the role of global SST. This is done in Feudale and Shukla (2010).

**Acknowledgements** We would like to thank O. Reale for his precious help in this research and J. Kinter and M. Fennessy for discussions and comments on this study. Thanks also to the Climate Dynamics department at George Mason University and COLA for providing access to their data set. This research was supported by the Research grant FISIR-CMCC (*Fondo Integrativo Speciale per la Ricerca* of the *Centro Euro-Mediterraneo per i Cambiamenti Climatici*).

## References

- Albuisson M, Delamare C, Leroy S, Wald L (2003) Heat wave of summer 2003 enhanced by cloudiness skies. Internal Report et the ECOLE DES MINES DE PARIS pp [http://www.soda-is.com/doc/canicule\\_eng.pdf](http://www.soda-is.com/doc/canicule_eng.pdf)
- Beniston M (2004) The 2003 heat wave in Europe: a shape of things to come? An analysis based on Swiss climatological data and model simulations. *Geophys Res Lett* 31:L02,202
- Black E, Sutton R (2007) The influence of oceanic conditions on the European summer of 2003. *Clim Dyn* 28:53–66
- Buzzi A, Tibaldi S (1978) Cyclogenesis on the lee of alps: a case study. *Q J R Meteorol Soc* 104:1542–1566
- Cassou C, Terray L, Phillips AS (2005) Tropical Atlantic influence on European heat waves. *J Clim* 18:2805–2811
- Chase TN, Wolter K, Sr PAP, Rasool I (2006) Was the 2003 European summer heat wave unusual in a global context? *Geophys Res Lett* 33. doi:10.1029/2006GL02799127,470
- Czaja A, Frankignoul C (2002) Observed impact of atlantic sst anomalies on the North Atlantic Oscillation. *J Clim* 15:606–623
- Della-Marta PM, Luterbacher J, von Weissenfluh H, Xoplaky E, Brunet M, Wanner H (2007) Summer heat waves over western Europe 1880–2003, their relationship to large scale forcing and predictability. *Clim Dyn* 29:251–275
- Fan Y, Van den Dool H (2004) Climate prediction center global monthly soil moisture data set at 0.5° resolution for 1948 to present. *J Geophys Res* 109:D10,102. doi:10.1029/2003JD004,345
- Ferranti L, Viterbo P (2006) The European summer of 2003: sensitivity to soil water initial conditions. *J Clim* 19:3659–3680
- Feudale L (2008) Large scale extreme events of temperature during 1950–2003. VDM Verlag, p 173, ISBN: 978-3-8364-8953-9
- Feudale L, Shukla J (2007) Role of Mediterranean SST in enhancing the European heat wave of summer 2003. *Geophys Res Lett* 34. doi:10.1029/2006GL027,991
- Feudale L, Shukla J (2010) Influence of sea surface temperature on the European heat wave of 2003 Summer. Part II: a modeling study. *Clim Dyn*. doi:10.1007/s00382-010-0789-z
- Fischer EM, Seneviratne SI, Vidale PL, Luthi D, Schar C (2007) Soil moisture–atmosphere interactions during the 2003 European summer heat wave. *J Clim* 20:5081–5099



- Goddard L, Mason SJ, Zebiak SE, Ropelewski CF, Basher R, Cane MA (2001) Current approaches to seasonal to interannual climate predictions. *Int J Climatol* 21:1111–1152
- Grazzini F, Viterbo P (2003) Record-breaking warm sea surface temperature of the Mediterranean Sea. *ECMWF Newsl* 99:2–8
- Huang B, Shukla J (2005) Ocean–atmosphere interactions in the Tropical and Subtropical Atlantic Ocean. *J Clim* 18:1652–1672
- Jung T, Ferranti L, Tompkins AM (2006) Response to the summer 2003 Mediterranean SST anomalies over Europe and Africa. *J Clim* 19:5439–5454
- Kalnay EM, Kanamitsu M, Kistler R, Collins W, Deaven D, Gandin L, Iredell M, White G, Woolen J, Zhu Y, Chelliah M, Ebisuzaki W, Higgins W, Janowiak J, Mo K, Joseph D (1996) The NCEP/NCAR 40-year reanalysis project. *Bull Am Meteorol Soc* 77:437–471
- Lutherbacher J, Dietrich D, Xoplaki E, Grosjean M, Wanner H (2004) European seasonal and annual temperature variability, trends, and extremes since 1500. *Science* 303:1499–1503
- Meehl GA, Tebaldi C (2004) More intense, more frequent, and longer lasting heat waves in the 21st century. *Science* 305:994–997
- Ogi M, Yamazaki K, Tachibana Y (2004) The summertime annular mode in the northern hemisphere and its linkage to the winter mode. *J Geophys Res* 109:D20,114. doi:[10.1029/2004JD004,514](https://doi.org/10.1029/2004JD004,514)
- Ogi M, Yamazaki K, Tachibana Y (2005) The summer northern annular mode and abnormal summer weather in 2003. *Geophys Res Lett* 32. doi:[10.1029/2004GL021,528](https://doi.org/10.1029/2004GL021,528)
- Reynolds RW, Rayner NA, T M Smith DCS, Wang W (2002) An improved in situ and satellite SST analysis for climate. *J Clim* 15:1609–1625
- Rowell DP (2003) The impact of Mediterranean SSTs on the Sahelian rainfall season. *J Clim* 16:849–862
- Schar C, Vidale PL, Luthi D, Frei C, Haberli C, Liniger MA, Appenzeller C (2004) The role of increasing temperature variability in the European summer heatwaves. *Nature* 427:332–336
- Smith TM, Reynolds RW (2004) Improved extended reconstruction of SST (1854–1997). *J Clim* 17:2466–2477
- Vautard R, Yiou P, D’Andrea F, de Noblet N, Viovy N, Cassou C, Polcher J, Ciais P, Kageyama M, Fan Y (2006) Summertime European heat and drought waves induced by wintertime Mediterranean rainfall deficit. *Geophys Res Lett* 34. doi:[10.1029/2006GL028,001](https://doi.org/10.1029/2006GL028,001)
- WHO (2003) Health effects of extreme weather events: WHO’s early findings to be presented at the World Climate Change Conference. [http://www.euro.who.int/mediacentre/PR/2003/20030929\\_1](http://www.euro.who.int/mediacentre/PR/2003/20030929_1)
- Xie P, Rudolf B, Schneider U, Arkin P (1996) Gauge-based monthly analysis of global land precipitation from 1971–1994. *J Geophys Res* 101:19,023–19,034
- Xoplaki E, Gonzalez-Rouco JF, Luterbacher J, Wanner H (2003) Mediterranean summer air temperature variability and its connection to the large-scale atmospheric circulation and SSTs. *Clim Dyn* 20:723–739